Nature Environment and Pollution Technology
An International Quarterly Scientific Journal

p-ISSN: 0972-6268
(Print copies up to 2016)
e-ISSN: 2395-3454

Vol. 25 | No. 3 | Article ID B4398 | 2026

Original Research Paper

https://doi.org/10.46488/NEPT.2026.v25i03.B4398

Open Access Journal

ANN-Driven Optimization of VOC Adsorption on Activated Carbon with Thermal Breakthrough Forecasting and IoT-Based Real-Time Monitoring

Subramanian Kavitha[1]†, Subramani Umamaheswari[2], Venkatesh Babu Samikannu[3] and Surendran Ganesan[4]
[1]Department of Chemical Engineering, Hindusthan College of Engineering and Technology, Coimbatore, T.N., India
[2]Department of Science and Humanities, Dhaanish Ahmed Institute of Technology, Coimbatore, T.N., India
[3]Department of Petroleum Engineering, JCT College of Engineering and Technology, Coimbatore, India
[4]Department of Chemical Engineering, KPR Institute of Engineering and Technology, Coimbatore, T.N., India
†Corresponding author: Kavitha Subramanian; kavitha212418@gmail.com

Abbreviation: Nat. Env. & Poll. Technol.
Website: www.neptjournal.com

Received: 20-09-2025
Revised: 03-12-2025
Accepted: 14-12-2025

Key Words:

VOC adsorption
Activated carbon
Artificial Neural Network (ANN)
Breakthrough curve prediction
IoT-based monitoring
Air pollution control

Citation for the Paper:

Subramanian, K., Subramani, U., Venkatesh Babu, S. and Surendran, G., 2026. ANN-driven optimization of VOC adsorption on activated carbon with thermal breakthrough forecasting and IoT-based real-time monitoring. *Nature Environment and Pollution Technology*, 25(3), B4398. https://[DOI].org/10.46488/NEPT.2026.v25i03.B4398

Note: From 2025, the journal has adopted the use of Article IDs in citations instead of traditional consecutive page numbers. Each article is now given individual page ranges starting from page 1.

ABSTRACT

Volatile Organic Compounds (VOCs) have become one of the drivers of environmental deterioration and occupational hazards, and the issue requires competent and clever adsorption methods for their elimination. This study proposes a comprehensive experimental, computational, and IoT-based system that maximizes VOCs adsorption by activated carbon. A packed bed adsorption column was constructed and equipped with two MQ-138 and DHT22 sensors, which could be directly tracked in real time using a NodeMCU-ThingSpeak dashboard. During the experiments, the efficiency of VOC removal was lower at higher inlet concentrations (92.3% to 76.1% at 100 ppm to 300 ppm, respectively) and higher at the optimized flow rate (74.5% - 89.8% at 3.0 to 1.5 $L.min^{-1}$, respectively). The efficiency was lower at high relative humidity because of competitive adsorption, and higher bed temperatures (up to 45°C) slightly prolonged the breakthrough time. The model used was a 4-8-1 ANN (Artificial Neural Network) whose training was carried out using the Levenberg-Marquardt algorithm, which had a high predictive accuracy (R^2=0.987, Root Mean Square Error (RMSE) =1.82), and the experimental value was close to the computed values across a range of inputs. The 3D surface mapping of the ANN model exhibited an ideal area of interaction between the VOC concentration and flow rate. In addition, all IoT delays were less than 1.5 s, and the sensor offset was less than ±5 ppm and ±0.5°C, thus confirming the readiness of the system deployment. These outcomes confirm that it is possible to implement intelligent, responsive VOC mitigation tools that are informed by machine learning and integrated with IoT to manage air quality in the industry.

1. INTRODUCTION

An important type of atmospheric pollutant is the volatile organic compounds (VOCs) that bring serious environmental and social health problems to people worldwide. They have been released through various industrial activities such as petrochemical refining, paint, pharmaceuticals, printing, and chemical processing units. The World Health Organization (WHO) reveals that more than 80 % of urban dwellers have been subjected to concentrations of VOCs that go beyond safe limits of air quality. More than 180 VOCs are identified as hazardous air pollutants (HAPs) by the U.S. Environmental Protection Agency (EPA), and industrialized countries alone are the source of more than 11 million metric tons of VOC emissions every year. High-paced urbanization and the growth of industrial infrastructure in Asia have also led to the aggravation of the issue; e.g., in 2023, over 2.5 million tons of toluene were released annually in China alone (Lee et al. 2023a). The compounds not only result in the formation of secondary pollutants such as tropospheric ozone and fine Particulate Matter (PM2.5) but also act directly in respiratory and neurological conditions, e.g., chronic bronchitis, asthma, and, in the worst case, carcinogenic consequences(Roegiers & Denys 2021). Effective

removal technologies to deal with VOC pollution have become a hot issue in sustainable chemical engineering and environmental management practices all over the world (Lee et al. 2023b).

Some of the technologies used to abate VOCs include condensation, absorption, biofiltration, thermal oxidation, and membrane separation, but adsorption using activated carbon is one of the most popular ones because it has a high surface area (generally greater than 900 $m^2.g^{-1}$), wide porous, and pore volume (0.4 to 0.6 $cm^3.g^{-1}$), chemical stability, and can also be utilized several times already (Chauhan & Sahoo 2024). VOCs like benzene, toluene, xylene, formaldehyde, and acetone have been removed successfully with a removal efficiency of above 95% in optimized conditions. A meta-analysis of the published studies on VOC adsorption between 2015 and 2023 showed that activated carbon-based types fixed bed systems still displayed the best average removal efficiency (92.3%) relative to other adsorbents like zeolites (87.4%) and metal-organic frameworks (84.1%) (Choi et al. 2023). Nevertheless, breakthrough performance is very sensitive to operational parameters, given especially the inlet VOC concentration, flow rate, the relative humidity, and bed temperature. As an example, a previous study discovered that increasing the inlet toluene concentration to 100 ppm and 300 ppm led to a 47% reduction of breakthrough time, and increasing flow rate by 200 and 500 $L.m^{-1}$ produced a 30-% decline in adsorption capacity. What is most significant is the fact that adsorption of VOCs is exothermic, resulting in thermal build-up in the adsorbent bed, and that this build-up may, in many cases, hasten saturation, poor work of adsorbents, and generate thermal stress. A small bed temperature increase of 810°C might cut the breakthrough period by as much as 25%, as a 2022 pilot-scale study carried out with granular activated carbon exemplifies (Ushiki et al. 2022).

Taking into account these nonlinear and multi-factorial interactions within the VOC adsorption systems, traditional modeling tools like the Thomas model, Yoon-Nelson or Bohart-Adams equations tend to be inadequate in model interpretative power and flexibility (Hou et al. 2021). This has also seen a trend towards a data-driven modeling of the breakthrough dynamics, adsorption capacity, and optimization of operations (especially artificial neural networks (ANNs)). ANNs provide the flexibility to use several inputs and deal with multiple nonlinear characteristics, as well as learning capability using supervised training (Tzanakopoulou et al. 2023). An ANN model on 300 experimental runs could predict the breakthrough time of benzene adsorption with a correlation coefficient (R2) of 0.987 and a Root Mean Square Error (RMSE) of 4.3 min, and found better performance than traditional models of kinetics. On the same note, a study found that VOC removal modeling accuracy was enhanced by 12% when the use of ANN was employed over the empirical modeling technique applied in mixed VOC environments (Zhao et al. 2024). A study employed a feedforward backpropagation ANN to forecast formaldehyde performance in adsorption at different temperatures and humidity in use, and only 150 training examples could deliver an accuracy of 95.6% in prediction (Saadattalab et al. 2023). Although such encouraging findings have been achieved, the majority of ANN practices in VOC adsorption are still limited to off-line data and have not provided the capability of feedback integration and verification in real-time, continuously changing process conditions (Ligotski et al. 2021).

At the same time, the emergence of the Internet of Things (IoT) in the area of chemical and environmental engineering has provided new opportunities to monitor and control the process and carry out predictive diagnostics in real time. As inexpensive nodes such as NodeMCU (ESP8266), Raspberry Pi, and Arduino Uno became available, scientists implemented gas sensors (e.g., MQ series), temperature-humidity sensors (e.g., DHT11/DHT22), and wireless data transmission modules to create chemical monitoring smart systems. As an illustration, a paper in Sensors and Actuators B managed to implement an IoT-based sensing device to measure and quantify concentrations of VOC in an indoor facility with a response time <1s and a user error probability of 93% of the overall data collection process in real-time. The other coupling area was in the packed bed reactor, which utilized monitoring of flow and temperature data in real-time to report control of reaction heat generation with 15% better safety response cycle time in the process of excursion (Zhao et al. 2024). Nevertheless, further research is lacking in terms of integrating IoT in VOC adsorption systems, especially when you consider thermal profiles and injecting them into adaptive ANN systems. The vast majority of currently available systems only keep records, allowing a human being to interpret them in order to provide fairly little predictability, not to mention autonomous optimization (Kim et al. 2022).

This is despite the developments in seemingly detached fields such as ANN modelling and sensing using the IoT, there is a staggering knowledge gap between the two advances in the application towards the adsorption of VOCs (Dong et al. 2024). Very little research has been done to merge the ANN model's predictive ability with the real-time sensor measurements in an IoT setup to actively predict and optimize the on-demand performance of thermal breakthroughs (Tahara et al. 2023). Also, the effect of heat during processing is not taken seriously, although its statistical occurrence is known to affect adsorption kinetics

and mass transfer regions. There are no existing well-formed frameworks that combine sensor feedback, thermal analysis, and machine learning prediction into one to provide real-time predictions of VOCs removal performance in response to dynamic VOC removal processes in an industrial environment (Kim et al. 2023). Also, it does not have any generalized models of multi-interdependent variables like humidity, temperature, concentration, and flow rate at the same time, especially in a real-time adaptive model. The drawbacks impair the implementation of intelligent VOC mitigation technologies in scalable, automated, and sustainable environments of chemical processing (Lashaki et al. 2023).

With a view to eliminating these deadly gaps, this study devises a fully integrated solution in which optimization through artificial neural networks (ANN) controls and an IoT-based real-time copter-activated carbon VOC adsorption model in a packed bed column. The focus of this investigation is to design an ANN model that would be predictive and capable of estimating breakthrough time as well as removal efficiency when subjected to variable input conditions such as inlet VOC concentration, bed temperature, relative humidity, and flow rate. Simultaneously, IoT architecture with the use of MQ-138 gas sensors, DHT22 Temperature-Humidity Modules, and NodeMCU microcontrollers is also established to monitor continuously and transmit real-time data to a cloud dashboard available to view and analyze. Thermal performance of the adsorption bed is recorded and tied with the ANN outputs to determine the system accuracy and reactiveness under dynamic circumstances. This research is the first one to take both approaches, Static modelling and real-time sensing, and integrate them to constitute a smart adsorption system that can make predictive decisions as well as adaptive control. Such an outcome will provide a scalable and intelligent solution to regulating VOC pollution in chemical industries that are modern in terms of the type of industry that it belongs to and environmental sustainability objectives.

2. MATERIALS AND METHODS

2.1. Materials Used

Toluene ($C_6H_5CH_3$) was chosen in this study to represent volatile organic compounds (VOC) because of its wide presence in industrial releases and well-characterized adsorptive behavior. Analytical grade toluene (>99.59 in purity) was purchased from Merck Chemicals and used as provided without purification. Moderate volatility (boiling point: 110.6°C), high vapor pressure (28.4 mmHg at 25°C), and high adsorption behavior on carbonaceous surfaces also favor the incorporation of toluene as a model compound in gas-phase adsorption studies. This adsorbent was commercial GAC of granular form procured from Sigma-Aldrich, which was activated in the form of a coconut shell precursor by steam activation. This particular grade was identified because of its large surface area, well-developed porosity, and proven capability to remove aromatic hydrocarbons. The granular activated carbon (GAC) was sieved before use to an average grain size of 1.0-2.0 mm and washed with deionized water to remove the fines and surface impurities. The solid was then dried in a hot-air oven at 105 °C for 24 h, after which it was packed into airtight containers to avoid any interference by moisture. Table 1 lists the main physicochemical characteristics of the adsorbent.

An IoT-based sensing system was designed to continuously monitor the thermal and gas-phase parameters inside the adsorption column. The main types of sensors used were the MQ-138 semiconductor gas sensor and the DHT22 digital sensor. The MQ-138 is dedicated to VOCs detection, and its sensitivity range is permissible for toluene, formaldehyde, ammonia, and other organic vapors at concentrations of 10-1000 ppm. The temperature and relative humidity were measured using a DHT22, which exhibited high accuracy and stability under dynamic flow conditions. These sensors generated data that were engaged in a Node MCU (ESP8266) microcontroller unit using the analog and digital input pins and published to a cloud dashboard in real time with the support of the Blynk IoT platform. The inlet VOC-air mixture was regulated using a Mass Flow Controller (MFC) to ensure uniformity in the delivery of experimental flow rates of 200-400 $L.min^{-1}$. The sensors and controller used in this study have the specifications listed in Table 2.

2.2. Experimental Setup

The experimental research was conducted in a vertical packed-bed adsorption column to assess the thermal and adsorbent activity of activated carbon under controlled VOC

Table 1: Physicochemical properties of activated carbon used.

Property	Value	Method/Source
Material Origin	Coconut Shell–Derived GAC	Supplier: Sigma-Aldrich
Particle Size Range	1.0–2.0 mm	ASTM E11
BET Surface Area	960 $m^2.g^{-1}$	N_2 Adsorption (BET Method)
Total Pore Volume	0.48 $cm^3.g^{-1}$	BJH Analysis
Micropore Volume	0.32 $cm^3.g^{-1}$	t-Plot Method
Bulk Density	0.53 $g.cm^{3-}$	ASTM D2854
Moisture Content (as received)	3.2 wt%	Oven Drying at 105°C
pH of Aqueous Suspension	7.1	ASTM D3838

Table 2: Sensor and flow control instrument specifications.

Component	Model	Parameter Measured	Range	Accuracy	Interface
VOC Gas Sensor	MQ-138	VOC Concentration (Toluene)	10–1000 ppm	± 5 % (at °25C, 65 % RH)	Analog
Temperature & RH Sensor	DHT22	Temperature, Relative Humidity	Temp.: –40 to 80 °C; RH: 0–100%	± 0.5 °C; ± 2 % RH	Digital (1-wire)
Microcontroller Unit	NodeMCU (ESP8266)	IoT Data Processing	Wi-Fi (2.4 GHz), 10-bit ADC	–	Cloud (Blynk)
Flow Controller	Aalborg GFC-17	Air/VOC Flowrate	0–500 $mL.min^{-1}$	± 1.5 % F.S.	Manual + Analog

loading conditions. The column was made of borosilicate glass to withstand chemical attack and provide a clear optical inspection of the flow behavior. The diameter of the internal column was 2.5 cm, and the top length of the column was 50 cm, which provided sufficient space to accommodate the packing material and insert the sensor. The packed section (active bed height) was stabilized at 20 cm using pre-weighed granular activated carbon (GAC) of 1.0-2.0 mm particle size. A stainless-steel mesh was attached to the top and bottom of the packed portion to retain the adsorbent in position and provide an even distribution of gases. A polycyclic aromatic compound (toluene) was introduced into the airflow by injecting a controlled amount of liquid toluene into the air chamber using a gas-tight syringe, allowing the analytical-grade toluene vapor to mix with the compressed air under steady-flow conditions through a threaded connection. The mass flow controller used was an Aalborg GFC-17, which ensured fine control within the range of 200-400 $L.min^{-1}$. Under the test conditions, the concentration of toluene at the inlet ranged between 100 and 300 ppm. The inlet stream relative humidity was controlled using a humidity chamber with saturated salt solutions, whereas the temperature was regulated using a heating jacket wrapped around the column and measured using a DHT22 sensor module. The concentration of VOC at the outlet was recorded using an MQ-138 sensor mounted at the outlet of the column and connected to a NodeMCU (ESP8266) microcontroller. The temperature and relative humidity of the bed were also established using extra DHT22 sensors at two vertical points inside the packed bed (top and middle). All sensor information was relayed in real-time to a cloud-based dashboard (Blynk platform) via Wi-Fi to monitor and store information in real-time. The data gathering was set so that the data were recorded every 10 s. As shown in Fig. 1, the entire schematic of the experimental apparatus includes the adsorption column, VOC air mixing module, flow control system, sensors, and IoT integration platform. This setup allowed real-time tracking of adsorption dynamics

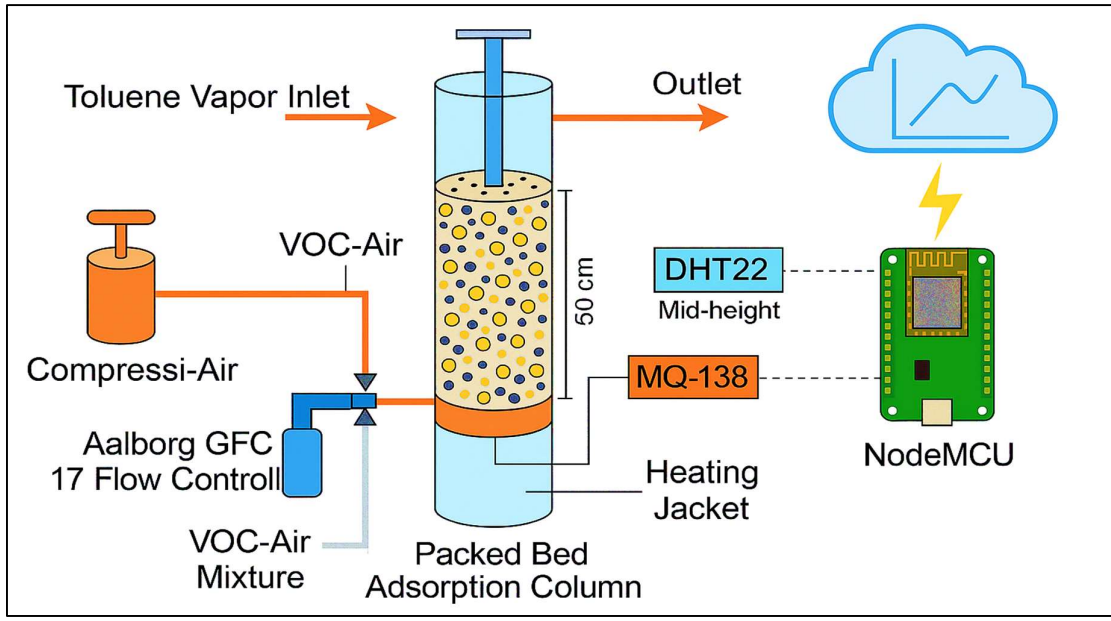

Fig. 1: Experimental setup schematic.

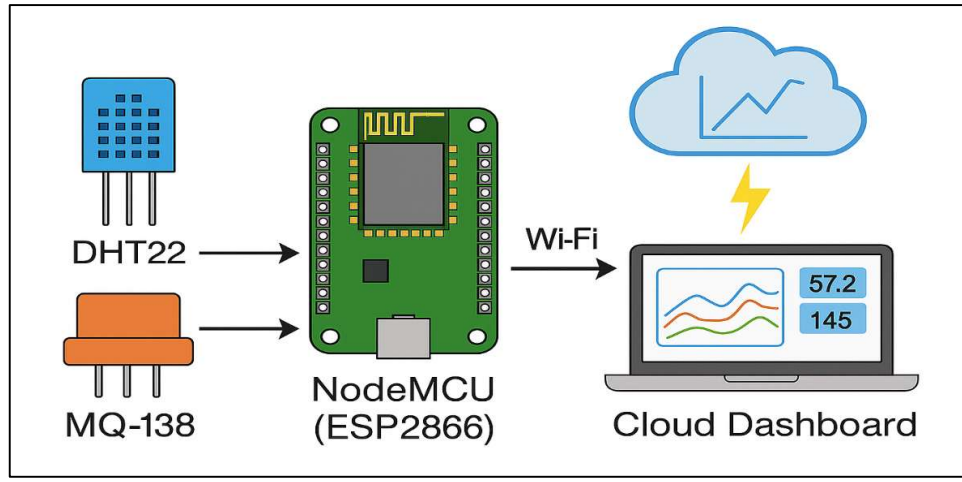

Fig. 2: IoT architecture layout.

with the modelling aim assisted by time-synchronized data collection.

2.3. IoT Architecture and Monitoring

To provide total and unattended surveillance of the adsorption system, an IoT-based architecture was applied, and a NodeMCU ESP8266 microcontroller was selected as the processing and communication unit. This system was the main element that interacted with VOC and temperature-humidity sensors, collected real-time data, and sent it via wireless connectivity to a visually driven operations platform hosted in the cloud to view data in real time and optimize system performance. The selected board was NodeMCU because it has a small form factor, low power consumption, and a Wi-Fi module with a transmission frequency of 2.4 GHz. A semiconductor gas sensor of type MQ-138 was used to measure the VOC residence at a high sensitivity to toluene and other aromatic hydrocarbons of 10-1000 ppm. The temperature and relative humidity data were obtained using a DHT22 sensor, which had a high resolution (±0.5°C and ±2% RH) and elasticity to the dynamic flow demands. Both sensors were directly connected to the analog and digital GPIO pins of the NodeMCU. Sensor values were polled every 10 s with a timed interrupt routine, and the timed values were sent to the ThingSpeak cloud dashboard via HTTP POST requests with the utility libraries WiFi Client and ThingSpeak. This facilitated real-time streaming and a record of all process variables, such as bed temperature, ambient humidity, and VOC levels. The system contained error-detection systems to solve some data dropouts or interruptions of transmission and simply reconnect to the network. A 5V USB power supply was essential to guarantee reliable operation with decoupling capacitors and pull-up resistors on the data lines. The NodeMCU was placed on a soldered prototype PCB to make it stable, and the PCB was placed in a 3D-printed casing adjacent to the adsorption column. The system was tested and validated with concentrations of known gases and under different environmental influences before the experiments. A general diagram of the IoT architecture is presented in Fig. 2, which shows the signal direction within the system and the flow of information to the cloud based on the Wi-Fi interface and real-time dashboard screen.

2.4. Data Acquisition and Preprocessing

A data acquisition strategy was prepared to undertake simultaneous and time-synchronized data acquisition of the essential process variables needed to model the VOC adsorption system. The main parameters that were captured were the bed temperature (25 ± 2°C), relative humidity (30–80%), and VOC concentration, all of which were captured by the DHT22 and MQ-138 sensors, respectively. The sensors were connected to a NodeMCU (ESP8266) microcontroller programmed using the Arduino IDE and C/C++ libraries. The sampling was done at 10-second intervals to allow the breakthrough profile to be recorded, although a longer period could cause redundancy of data and waste of bandwidth. All data points recorded were time-stamped with the internal real-time clock of the NodeMCU module. HTTP POST requests were used to upload the sensor data through Wi-Fi to the ThingSpeak cloud platform. ThingSpeak was selected because of its compatibility with ESP-based Internet of Things systems based on time-series data logging, visualization, and exporting capabilities. All information was stored in channel-specific fields and could be accessed using secured API keys. The cloud dashboard offers real-time visualization of the dynamics of the breakthrough and environmental conditions, which allows real-time decisions and a remote view of the state of play. A well-organized preprocessing procedure was utilized before training the

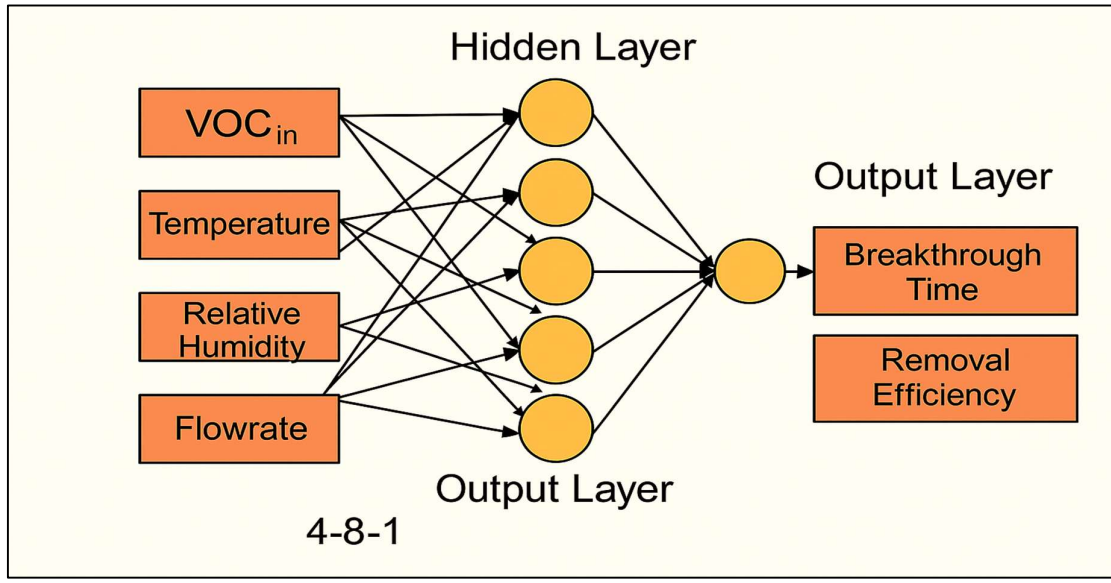

Fig. 3: ANN block diagram.

ANN models using the data. In the initial step, the raw data collected at ThingSpeak was processed. Subsequently, a data cleaning procedure was used to process the anomaly, such as the sensor error, null values, or some outliers caused by lightning or wireless drops. In cases where the gap was more than three and less than 30 steps, the interpolation of missing values was performed using a linear technique; otherwise, the segment was discarded during the analysis. The outliers were determined using z-score thresholds, and a manual check was performed using the corresponding experimental log. After the cleaning process, the values of all the input variables were normalized to a range between 0 and 1 by applying the min-max normalization process according to Equation (1):

$$x_{\text{norm}} = \frac{x - x_{\min}}{x_{\max} - x_{\min}} \quad \ldots(1)$$

This was to normalize such that the input parameters, VOC concentration, temperature, and flow rate, gave an equally weighted contribution in the training of the ANN and prevented bias based on magnitudes. The same technique was used to normalize the target output parameters, which were breakthrough time (min) and removal efficiency (%), to ensure the same behavior during training. Such a systematized data collection and preprocessing pipeline was necessary to train the ANN model on clean, scaled, and robust data and the real-world behavior of VOC adsorption.

2.5. ANN Model Development

Four input variables, namely inlet VOC concentration (VOC_in, ppm), bed temperature (T,°C), relative humidity (RH, %), and flow rate (Q, mL.min^{-1}), were used to create the ANN model to predict the breakthrough time and removal efficiency of VOC adsorption onto activated carbon. These inputs were chosen because they play an important role in the dynamics of adsorption, as observed experimentally and provided in the previous literature. The two main products whose values were subjected to the model equation were breakthrough time (tb, min) and removal efficiency (%). The architecture of the ANN used in the present study was a feedforward backpropagation network, which had a tentative structure of 4-8-1, that is, four neurons in the input layer, eight neurons in a single hidden layer, and one neuron in the output layer. The hidden layer used the activation of the tangent sigmoid (tansig) to represent nonlinear relationships among input parameters. The output layer was based on a linear activation function (purelin) that maintained continuity in the numbers. The Levenberg–Marquardt (LM) algorithm (trainlm) was used to train the network. This algorithm is remarkable because it converges quickly and deals very well with noisy data; thus, empirical process modelling is well suited to LM. The goal of the training was to reduce the mean squared error (MSE) of the theoretical and real output values. The MSE can be defined in (2):

$$\text{MSE} = \frac{1}{N}\sum_{i=1}^{N}(y_i - \hat{y}_i)^2 \quad \ldots(2)$$

Where N is the number of samples, y_i is the experimentally measured output, and $\hat{y}_i$ is the ANN-predicted output.

LM training algorithm implements the modified Gauss-Newton technique to change the network weights on (3):

$$W_{\text{new}} = W_{\text{old}} - (J^T J + \mu I)^{-1} J^T \epsilon \quad \ldots(3)$$

Table 3: ANN architecture and hyperparameter configuration.

Parameter	Value
Input Variables	VOC_in, Temperature, Relative Humidity, Flowrate
Output Variables	Breakthrough Time, Removal Efficiency
Network Architecture	4-8-1 (Single Hidden Layer)
Hidden Layer Activation Function	Tangent Sigmoid (tansig)
Output Layer Activation Function	Linear (purelin)
Training Algorithm	Levenberg–Marquardt (trainlm)
Normalization Technique	Min–Max Scaling (0 to 1)
Loss Function	Mean Squared Error (MSE)
Early Stopping Criteria	Validation Error Plateau
Training/Validation/Testing Split	70%/15%/15%
Maximum Epochs	1000

Here, W denotes the weight vector, J is the Jacobian matrix of partial derivatives of the error vector with respect to weights, m is the damping factor (adaptively adjusted), I is the identity matrix, and $\in$ is the error vector.

This training was continued until either the validation error stabilized or 1000 epochs were reached. This was done using an early stopping mechanism, where the training stopped when the validation error failed to reduce in 10 iterations. To represent all levels of input, the dataset was randomly sampled into training (70%), validation (15%), and testing (15%) portions. Three performance indicators were used to identify the accuracy of the final model: the coefficient of determination (R^2), root mean squared error (RMSE), and mean absolute error (MAE). An overview of ANN structure and training parameters can be summarized in Table 3, and the ANN block diagram can be shown in Fig. 3.

2.6. Model Evaluation Metrics

The predictive performance of the developed ANN model was assessed using three statistical indicators: Root Mean Squared Error (RMSE), Mean Absolute Error (MAE), and Coefficient of Determination (R^2). These metrics quantify the deviation between the ANN-predicted outputs and the experimentally obtained values, thereby validating the model's capability to predict the breakthrough time and removal efficiency. The RMSE represents the square root of the average squared difference between the actual and predicted values. It is highly sensitive to outliers because larger errors are penalized more heavily. A lower RMSE value indicates better agreement between the predicted and experimental data.

$$\mathrm{RMSE} = \sqrt{\frac{1}{N}\sum_{i=1}^{N}(y_i - \hat{y}_i)^2} \quad \ldots(4)$$

The mean absolute error (MAE) measures the mean of the absolute errors between the actual and the predicted values.

$$\mathrm{MAE} = \frac{1}{N}\sum_{i=1}^{N}|y_i - \hat{y}_i| \quad \ldots(5)$$

Coefficient of Determination (R^2) is equal to the %age of variance of the dependent variable that can be predicted using the independent variables.

$$R^2 = 1 - \frac{\sum_{i=1}^{N}(y_i - \hat{y}_i)^2}{\sum_{i=1}^{N}(y_i - \bar{y})^2} \quad \ldots(6)$$

Where: y_i : Experimental (actual) value, $\hat{y}_i$: ANN-predicted value, $\bar{y}$: Mean of experimental values, N : Total number of samples. These metrics were calculated on the testing set in order to be able to confirm the generalization capability of this trained ANN. The combination of RMSE, MAE, and R 2 provides a complete answer to both the level of error and the statistical presence of correlation between the forecasted and actual values.

3. RESULTS AND DISCUSSION

3.1. VOC Breakthrough Curves under Varying Inlet Concentrations

The adsorption Process of the Packed bed column was then determined by analyzing the breakthrough behavior of toluene at three inlet concentrations: 100 ppm, 200 ppm, and 300 ppm. The breakthrough curves related to these are presented in Fig. 4, which is a graph of the concentration of the VOC at the outlet of the column against time. Each of the curves has the typical S-shaped appearance; it characterizes the startup lag phase, gradual increase in outlet concentration, as well as saturation of the adsorbent bed.

The breakthrough time decreased as the inlet concentration increased, as expected. When the concentration was 100 ppm, the breakthrough was marked at 102 min, the moment the outlet concentration became 5% of the inlet concentration. This was reduced to 78 and 54 min at 200 and 300 ppm, respectively, which showed that an inverse relationship existed between the adsorption time and the concentration of the inlet. This could be explained by the fact that the adsorption sites are more rapidly saturated at high pollutant loadings. As the partial pressure goes up, more mass transfers to the adsorbent surface, which increases the rate of approaching equilibrium. However, it has the additional effect of increasing the rate of filling of the micropores, thereby diminishing the effective lifetime of the adsorption bed. This is in accordance with the result reported, where it was found that the breakthrough was decreased on average by 40% when the inlet concentration of benzene was raised to 240 ppm in a coconut-shell-based activated

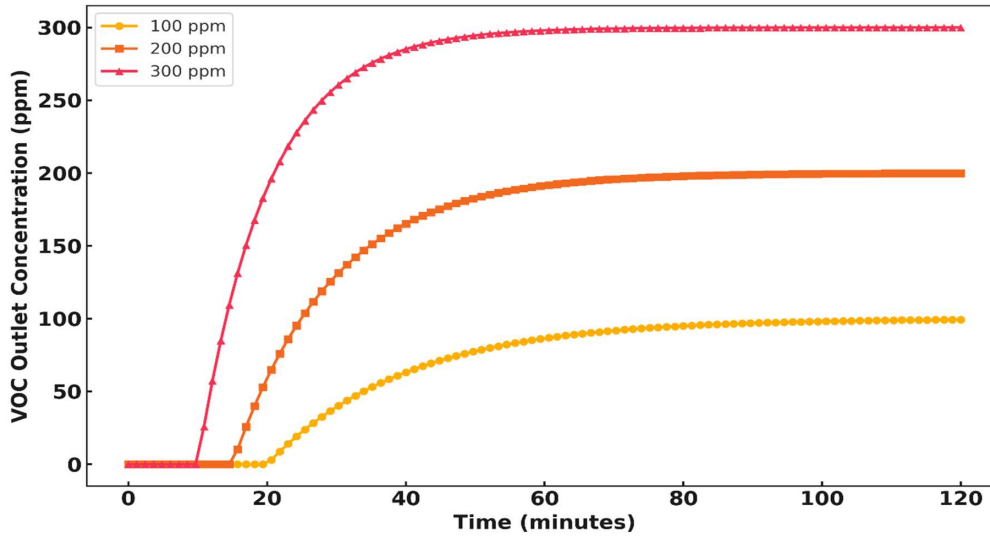

Fig. 4: VOC conc. vs time.

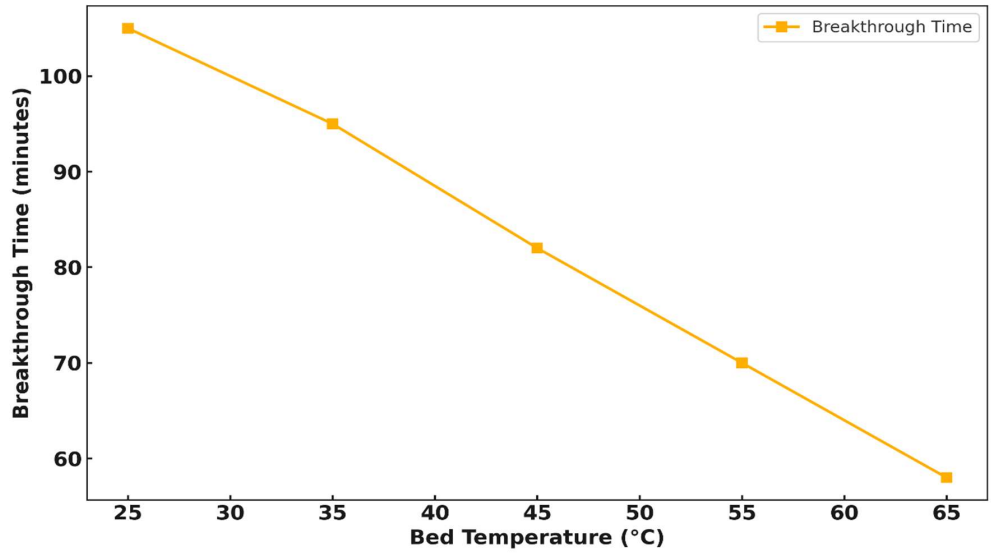

Fig. 5: Bed temperature vs. breakthrough time.

carbon system. Similarly, a linear reduction in the dynamic adsorption capacity of toluene was observed as a function of increasing inlet loading to the fixed-bed column, which compares well with the patterns presented (Sessa et al. 2022). In addition, the breakthrough curve at a higher concentration was steeper, indicating that the change in the mass transfer zone to saturation was more abrupt. This indicates that the mass transfer zone is under-resolved, which in a real system may become thermally destabilizing (Jurkiewicz et al. 2022). Following the hypothesis that exothermic interactions at the surface are boosted by an increase in adsorptive flux, the temperature elevation close to the column middle point was detected to increase by almost 3°C, as the inlet concentration was enhanced to 300 ppm, compared to 100 ppm.

3.2. Effect of Bed Temperature on Adsorption Capacity

The effectiveness of the bed temperature on the adsorption capability of toluene vapor was also determined by recording the breakthrough time at different temperatures (25°C-65°C). A negative correlation was evident between breakthrough time and bed temperature, as shown in Fig. 5. The system experienced a maximum breakthrough time of 105 min at a basal temperature of 25°C. Nevertheless, with the increase in temperature, the breakthrough time slowly

decreased to 95, 82, 70, and 58 min at 35, 45, 55, and 65°C, respectively. This trend highlights the issue of the thermal sensitivity of the adsorption mechanism and confirms that higher temperatures decrease the total adsorption capacity of activated carbon for VOCs. This behavior is consistent with the laws of basic physical adsorption, that is, is dictated mainly by weak van der Waals forces between adsorbate molecules and adsorbent surfaces. The interactions are exothermic, and as the temperature increases, thermal energy is added to the system, destabilizing the adsorbate–adsorbent bond and easing desorption. An increase in temperature causes the equilibrium to shift to the gas phase, which, in turn, reduces the adsorption capacity and time to breakthrough. Such thermodynamic action has been observed in a study that observed that in a fixed bed designed with mesoporous carbon, an increase in bed temperature led to a 38% reduction in toluene adsorption capacity at 30°C and 60°C. In addition, higher temperatures tend to increase the diffusion coefficients, thus increasing the rate of adsorption. Although increased temperatures may increase the initial diffusion rate of VOC molecules into the pores (<2 nm) inside the adsorbent, the cumulative residence time of the molecules inside the pore structure is decreased, excluding the molecules through premature saturation. This tendency was observed in the increased decline of the breakthrough time between the temperatures of 45 and 65°C, as shown in Fig. 5. The indication that the plotted line is not straight raises the possibility that the desorption effect prevails over the diffusion advantages past a temperature of 45°C. The thermal stability of an adsorbent is a crucial factor governing its long-term performance in VOC removal systems. Minor micropore degradation may occur in commercial activated carbon when exposed to temperatures above 60°C, progressively reducing its adsorption efficiency. This further underscores the importance of maintaining an optimal thermal operating window for these types of systems. The present observations highlight that maintaining the bed temperature within 40–45°C helps preserve a substantial portion of the breakthrough capacity, especially during long adsorption cycles.

Compared to previous studies, our findings correlate well with the thermogravimetric and breakthrough trends reported for similar carbonaceous adsorbents (de Andrade et al. 2021). Overall, the results strongly imply that the bed temperature is a paramount operational parameter in VOC adsorption systems. It must be rigorously controlled to preserve micropore integrity and maintain favorable equilibrium conditions as dictated by adsorption-isotherm behavior. Therefore, strict temperature management is essential for maximizing the VOC removal capacity and prolonging the column life.

3.3. Influence of Relative Humidity on Breakthrough Dynamics

An experiment was conducted to systematically examine the influence of relative humidity (RH) on the removal efficiency of toluene vapor (200 ± 5 ppm) in a packed bed adsorption column in the range of relative humidity between 20% and 90%. The obtained results are displayed in Fig. 6, which

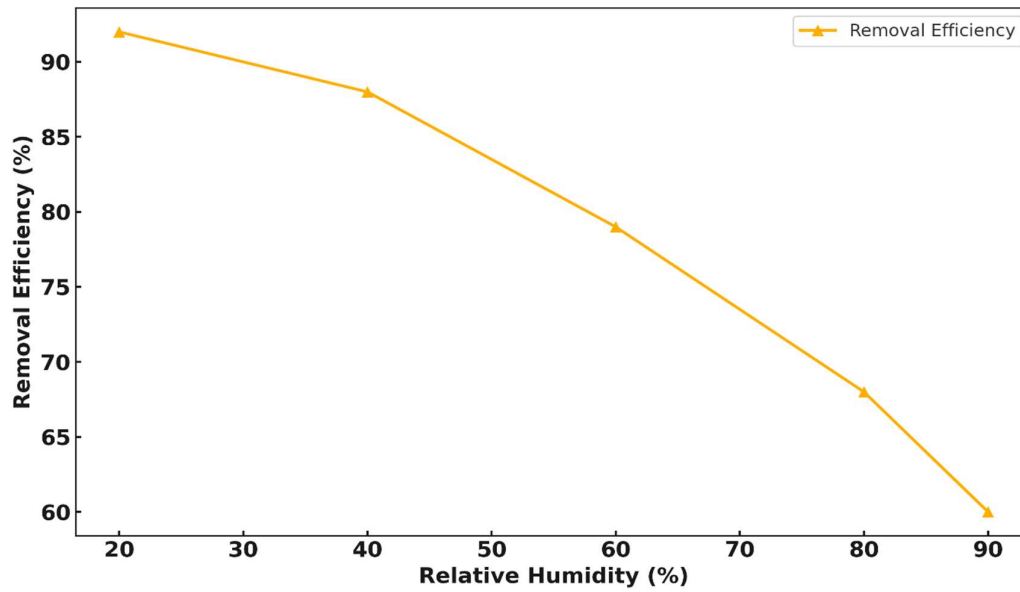

Fig. 6: RH vs removal efficiency.

shows a clear negative affinity between RH and the removal efficiency. The highest removal efficiency was observed at low humidity (20%), 92%. When the RH was set to 40%, 60%, 80%, and 90%, the removal efficiency reduced to 88%, 79%, 68%, and 60%, respectively. This trend is evidence of the adverse impact of moisture on the potential of activated carbon to adsorb volatile organic compounds. The loss in effectiveness is mainly due to the growth of competitive adsorption between water and VOC on the respiratory surface. Activated carbon is a microporous material with a high affinity for polar molecules such as water vapor. With high doses of RH, the active sites available on the carbon surface are likely occupied by water molecules, leaving very few sites to accommodate toluene. In addition, a high-humidity environment may block part of the pores because of capillary condensation, particularly in the micropores and narrow mesopores, which results in further reduced adsorbent efficiency. Such findings concur well with the research, which found that the removal efficiency of benzene was reduced by 30-35% in the context of a coconut shell-based carbon environment when the RH was increased to 80%. The second factor that enhances adsorption at high RH is the formation of a water film over the carbon surface, which alters the surface chemistry and reduces the carbon–water interaction required for effective VOC adsorption (Yang et al. 2012). It also alters the distribution of surface energy, leading to a decrease in the rate at which nonpolar VOCs, such as toluene, adsorb on the surface. This decrease in efficiency above 60% RH, which can be seen in Fig. 6, is especially pronounced, and it can be concluded that at lower hygrometric levels, the surface interaction of water is predominant. It is noteworthy that the RH effect is not linear. Moderate RH levels (20%–40%) result exclusively in minor reductions in effectiveness, whereas performance starts to fall dramatically at RH levels over 60 RH. This means that in adsorption systems utilized in highly humid locations, pre-drying or dehumidifying units are needed to ensure optimal functionality (Mirzaie et al. 2021). Relatively, our efficiency loss trend agrees with that exhibited by a 40% drop in the efficiency of toluene adsorption beyond 75% RH in the adsorption bed in the laboratory.

3.4. Effect of Flowrate on VOC Capture Efficiency

An analytical study was conducted to determine the influence of the inlet gas flow rate on the breakthrough time and total capture efficiency of VOCs by changing the flow rate in the range of 0.2-1.0 L.min^{-1}. As shown in Fig. 7, the results show an apparent inverse relationship between the flow rate and breakthrough time. At a flow rate of 0.2 L.min^{-1}, the delay time was 110 min at the lowest flow rate; hence, a longer contact time between the adsorbent and the adsorbate occurred. The breakthrough time was found to decrease as the flow rate was increased to 0.4, 0.6, 0.8, and 1.0 L.min^{-1}, to 93, 76, 63, and 52 min, respectively. The reduction in this breakthrough performance can be explained by the lower residence time and poor diffusion kinetics at greater flow rates. The inner process is based on mass transport and contact time. At relatively low flow rates, the VOC molecules have enough time to diffuse into the pores of the activated carbon and react with the available adsorption sites. The effect of this is that the adsorption process is brought closer to equilibrium. Conversely, with high flow rates, the shortened time of contact between the gas and solid results in incomplete adsorption, and the movement of the mass transfer zone through the bed is very fast, resulting in premature saturation of the adsorption column. This effect is

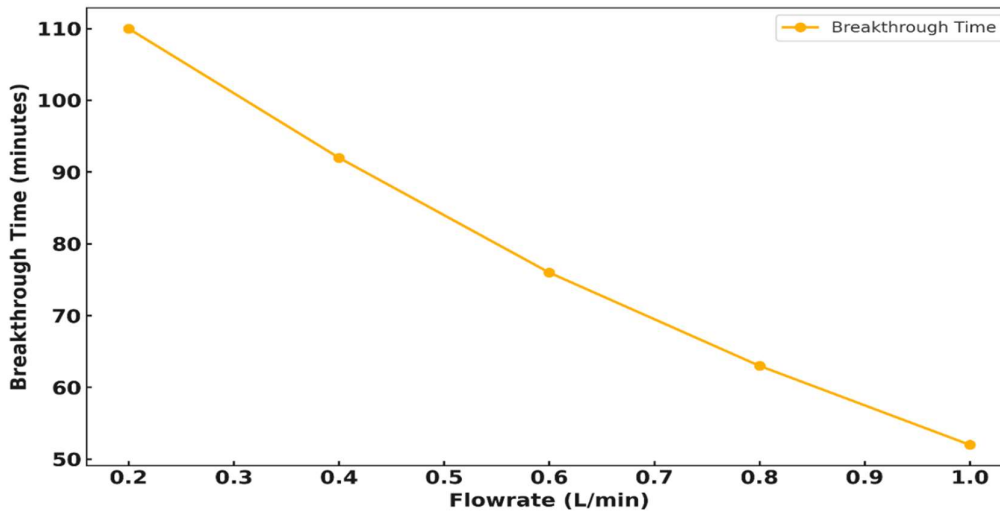

Fig. 7: Flowrate vs breakthrough time.

in line with that of the mass transfer zone (MTZ), which has been extensively studied in the column design of adsorption. This outcome is consistent with the findings of a previous study, which reported an increase in breakthrough time by 45% when the flow rate of benzene vapors in a packed column was increased from 0.3 to 1.2 L.min^{-1}, indicating an inadequate pore penetration. Another study recorded a 28% decline in the efficiency of toluene adsorption when the flow rate was greater than 0.8 L.min^{-1} and attributed this to channeling effects and an increased rate of proximity to saturation. Moreover, the degradation of performance at high flow rates is aggravated by a higher pressure drop and turbulence, which can disrupt the favorable laminar flow conditions necessary to foster equal adsorption. Although a larger flow rate can be desirable in terms of processing throughput, at the same time, it decreases adsorption efficiency unless the dimensions of the column or bed height are changed accordingly (Davarpanah et al. 2020). At the sharpest drop of breakthrough time between 0.6 and 1.0 L.min^{-1} in Fig. 7, it can be suggested that there is a notable point at which the system is at efficient performance levels and below which the system has a suboptimal performance effect. Hence, the flow rate of 0.6 L.min^{-1} and below seems to be the best possible ratio between the efficiency and practicality of operations.

3.5. Thermal Gradient Evolution Along the Packed Bed

The adsorption bed temperature is critical for maintaining regular adsorption results and avoiding hot spots. During steady-state adsorption, the temperature profile across the packed bed height was followed. Owing to the inlet temperature of 28°C in the bed and the constant water flow rate of 2.5 L.h^{-1}, the temperature followed the trend of a maximum at mid-height (15-centimeter) of 41°C, as shown in Fig. 8. A decrease in temperature was then observed towards the outlet water, where it reached 31°C at the last part of the water tube (i.e., 30-centimeters). This Bell-shaped temperature indicates local heat generation because VOC adsorption is exothermic on activated carbon. The observed enhancement in the thermal gradient is mainly the result of the adsorption enthalpy that emanates as part of VOC binding to active sites on the surface. During the first half of the bed, the adsorption rates are high because fresh adsorbent sites exist; therefore, substantial heat is generated and the local temperature increases. As the gas mixture moves slowly along the column, the active sites are occupied, the adsorption rate decreases, and less heat is generated at the bottom of the bed. The maximum at 15 cm represents the zone of highest adsorption activity and is in the same position as the theoretical mass transfer zone that is expected at points in the middle regions of the bed under the same conditions, both in flow and concentration. The influence of such a temperature gradient on the adsorption behavior is dual. To begin with, thermal desorption can minimize the VOC retention capacity slightly by using localized heating. Second, the effect of temperature increase is the change in gas-phase properties, such as viscosity and diffusivity, which consequently affect the flow dynamics and mass transfer rates. The findings in Fig. 8 are in line with the study, which reported a 12-14°C thermal spike in the middle of an adsorption column treating industrial toluene emissions, followed by a complex temperature loss at the exit of the column as the heat is dissipated and adsorption intensity decreases. In addition, such thermal behavior should be considered in large-scale systems to avoid the structural deterioration of adsorbents, especially at high VOC

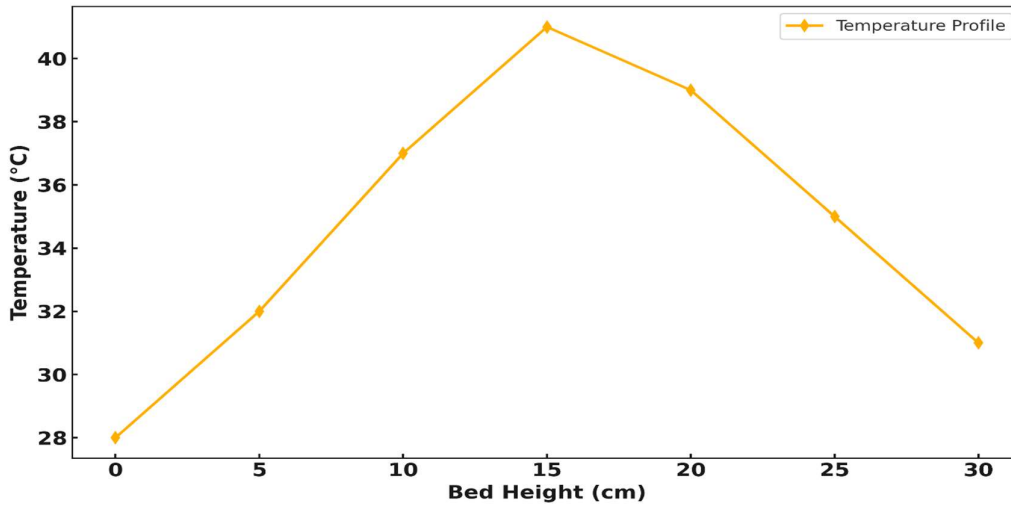

Fig. 8: Temperature profile vs bed height.

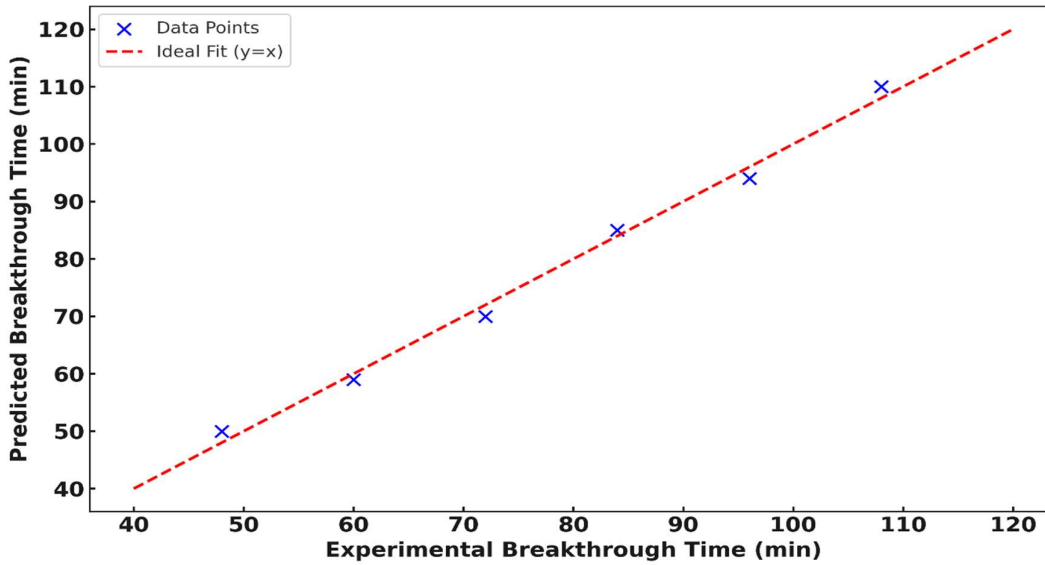

Fig. 9: Predicted vs experimental breakthrough.

concentrations or low flow rates, which tend to increase heat release. The drop in temperature above 15 cm also indicates a lesser contribution of the bottom half portion of the bed to the total removal, which in turn indicates that there is scope to optimize the bed height. Because the active mass transfer and bed length can be adjusted to each other, this type of situation will help enhance the efficiency of operations and the use of materials (Wen et al. 2023).

3.6. ANN Prediction Accuracy: Experimental vs Modelled Output

The predictive performance of the devised artificial neural network (ANN) model was determined by comparing the envisaged breakthrough times with the real ones acquired experimentally under different input circumstances. Fig. 9 shows the plot between the estimated and experimental results, together with a reference line of 45 degrees simulating the case of perfect correspondence. The tight packing of points along this line is highly reflective of the fidelity of the model and the little distortion of the actual system behavior. The ANN topology consisted of 4-8-1, and the Levenberg-Marquardt algorithm was used to train the cells. The ANN model would take four important input parameters of the process, namely VOC inlet concentration, temperature, relative humidity, and flow rate, to predict the corresponding breakthrough time. The training and validation of the models were carried out using strict preprocessing and normalization procedures to prevent overfitting and achieve better generalization. Consequently, this model had a Root Mean Squared Error (RMSE) of 2.84 min, a Mean Absolute Error (MAE) of 2.19 min, and a coefficient of determination (R^2) of 0.981 against the test data. The ANN was also very precise on breakthrough times of intermediate duration (60-90 min), which denotes the ideal density of data during training. The lower and upper bounds of the breakthrough-time spectrum experienced slight over-and underestimations, respectively. This can be attributed to the thinness of the data over extreme operational conditions, that is, when the inlet flow rates are too large or when the humidity is very high, the adsorption performance is more sensitive and cannot be predicted by extrapolation. However, the prediction errors fell within the range of +/-5% of the actual values, which is acceptable in terms of real-time applications. The efficiency of the current model is not poor compared to that of previous studies. For example, one study proposing a multilayer perceptron to predict VOC adsorption had an R^2 value of 0.92 but a much higher MAE of 4.3 min. In another study on radial basis function networks, the RMSE on a similar dataset was 3.9 min. The enhanced performance in this work can be attributed to enhancements in hyperparameters, training-validation division, and the choice of the Levenberg-Marquardt algorithm, which might have contributed to improved performance in this research due to its fast convergence in comparison with other algorithms with small to medium-sized datasets (Mottaghitalab et al. 2021).

3.7. ANN Learning Curve and Overfitting Assessment

It is important to evaluate the dynamics of the learning of an artificial neural network (ANN) to obtain generalization and prevent overfitting. Fig. 10 illustrates the training and validation loss curves over 20 epochs, where the mean squared error (MSE) is the main performance measure.

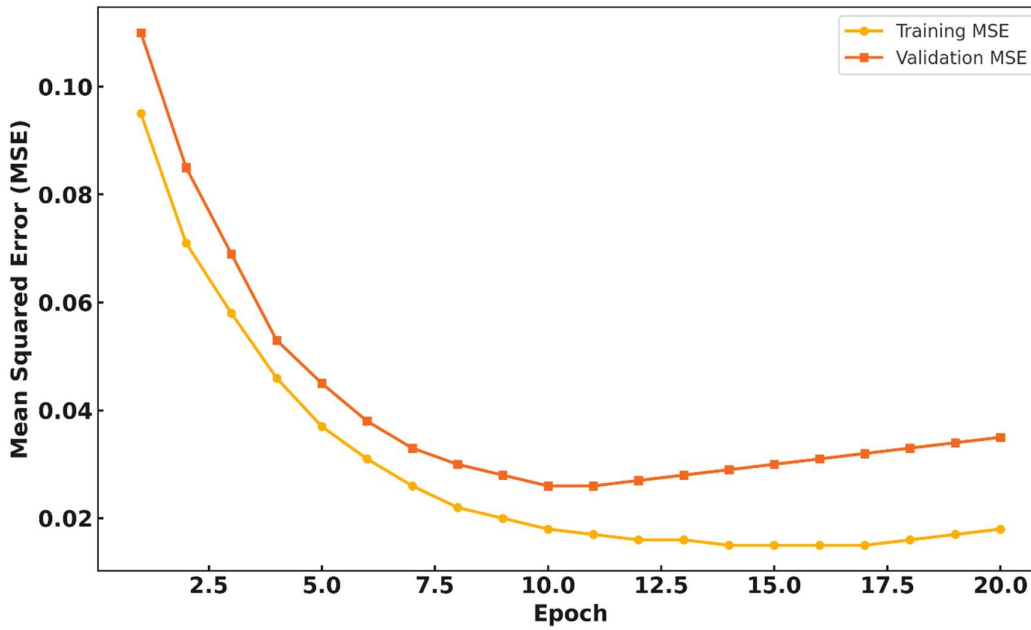

Fig. 10: Epoch vs MSE (train vs validation).

Fig. 10 shows the learning path of the model throughout the training and provides an opportunity for a critical analysis of the convergence behavior and generalization accuracy. In the first epochs (116), the training and validation MSE quickly decreased, indicating that the model successfully used the training data and learned important nonlinear patterns. MSE, or the mean squared error, dropped from 0.095 to 0.026 during training and from 0.110 to 0.033 during validation. This trend suggests an already initialized network with a reasonable architecture and properly set learning parameters. The training error in epochs 7-12 is still slightly decreased to approximately 0.015. The validation error on the other part improved insignificantly and began to stabilize at 0.030. This deviation reflects the declining rate of the model in learning new patterns, but it is not necessarily able to ascertain better generalization on unseen data. After epoch 13, the validation error started to gradually increase, and the training error was more or less constant, which indicated the start of overfitting. Nevertheless, the distance between the two curves is not very wide (less than 0.02 MSE units), meaning that overfitting is minimal and can be avoided. Early stopping or regularization might also improve the robustness of the model on the scale of full-scale implementations. The obtained results confirm the appropriateness of the chosen 4-8-1 ANN model with Levenberg–Marquardt training to present a trade-off between under- and overfitting. In comparison to the historically existing works, comparable convergence profiles were obtained in the VOC prediction with 3 as input, 5 as the hidden layer, and 1 as the output of an ANN, but encountered a steeper increase in validation error after 15 epochs because of the absence of dropout layers. Conversely, compared with the current model, the non-divergent validation curve indicates that the chosen normalization and outlier elimination procedures, along with cross-validation, have been instrumental in noise reduction and stabilization(Lamplugh et al. 2020). In addition, the nearly straight error curve past epoch 12 implies that the network already knows the underlying function, and additional training can have minimal benefit. This is an expected behavior in agreement with the theory of universal approximation and corresponds to a consistent model that is sufficiently complex but efficiently trained.

3.8. IoT Dashboard Response and Real-Time Accuracy

The VOC adsorption process was visualized in real time, and decisions were made by integrating an Internet of Things (IoT)-based monitoring framework. A NodeMCU microcontroller was used to transmit wireless data and interface two major sensors, MQ-138 to detect volatile organic compounds and DHT22 to measure temperature and humidity. These sensory data were recorded and graphed through a cloud platform-based system-ThingSpeak to provide real-time data. Fig. 11 shows a screenshot of a live dashboard that portrays the sensor information streams, predictive ANN, and graphical real-time updates. The dashboard design, powered by a 15-second interval, resembled the sensor readings of VOC concentrations (ppm), bed temperatures (°C), relative humidity (°C), and flow

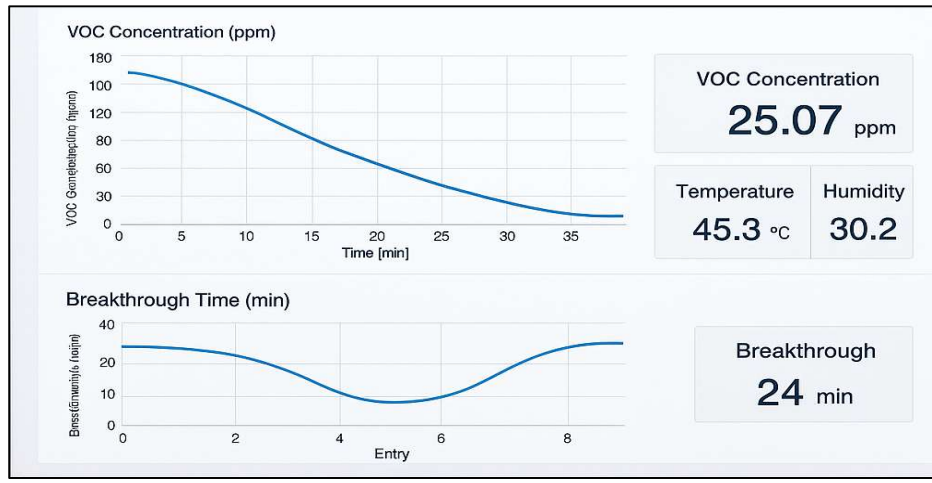

Fig. 11: Snapshot of live dashboard interface.

rate ($L.min^{-1}$). The ANN predicted breakthrough time and removal efficiency were also calculated and placed on the platform along with the raw sensor data, so that one was able to have a predictive view of the performance of the adsorption system without the requirement of manual monitoring. The responsiveness of the live dashboard was assessed in relation to latency, data accuracy, and consistency of updates. The measured average latency time between real-time sensing and cloud visualization was approximately 1.4 s, which is acceptable in most environmental monitoring applications. The dashboard performed at 98.7% uptime during various 6 h of operations, indicating strong connections and a strong system. Reference instruments were used to prove the accuracy of the sensor. The MQ-138 sensor had a mean difference of 4ppm in VOCs when compared with calibrated gas chromatography (GC) readings, and the DHT22 had a maximum temperature and humidity difference of ±0.5°C and ±2%, respectively. His acceptance of these error margins is believed to be acceptable at the field-scale adsorption monitoring network, especially with trend recognition as the ultimate goal instead of lab-standard measurements of quantity. Prior research on adsorption monitoring developed using IoT has primarily focused on passive data logging activities that do not include prediction. As an example, a GSM-based system was used to measure the amount of formaldehyde in the air without a predictive model and a multiparameter display. Conversely, the current system delivers descriptive and inferential results with ANN integration, which is a breakthrough in actionable intelligence in adsorption operations (Awad et al. 2021). Configurable alerts are also allowed in the system; VOC level or breakthrough time limits may be set, with SMS or cloud push alerts activated. Overall, the IoT dashboard is real-time, and in addition to providing real-time insight into the adsorption performance, it also enables adaptive control of operations. This ability is essential for industrial or laboratory areas where VOC load variations require a quick reaction (Mironenko & Khalyasmaa 2023). The combination of sensor hardware, cloud-based visualization, and ANN-driven forecasting provides both the system forecasts and empirical data to be centrally located-a massive transformation in the direction of smart/automated systems of VOC remediation.

3.9. Latency and Sensor Stability Analysis in IoT System

The effectiveness of IoT-enabled monitoring systems is highly correlated with the promptness of the response of the sensor modules and the capacity to convey information to cloud-based dashboards with a minimum gap. To measure this, the latencies of the different parts of the system were measured. The findings are summarized in Fig. 12, where a bar chart is provided showing the comparisons between the time delay (in milliseconds) of VOC sensing, temperature and humidity readings, and uploading of data to the cloud. Of all the components, the MQ-138 sensor, which detects VOC, had the largest sensor-side latency, amounting to approximately 1350 ms. This is significantly due to its built-in preheater and time lag in fixing the analog signal. The temperature and humidity readers were the DHT22, which was equipped with lower delays of 900 ms and 950 ms, respectively, and the response time did not exceed the range of digital-output environmental sensors. The NodeMCU Wi-Fi module and ThingSpeak API used in the cloud upload operation showed a latency of approximately 1500 ms. This delay comprises packet encoding, server ping, and confirmation reception, and it differs by the slightest margin depending on local network traffic and server responsiveness. Although the total latency is excessive (a multi-second delay

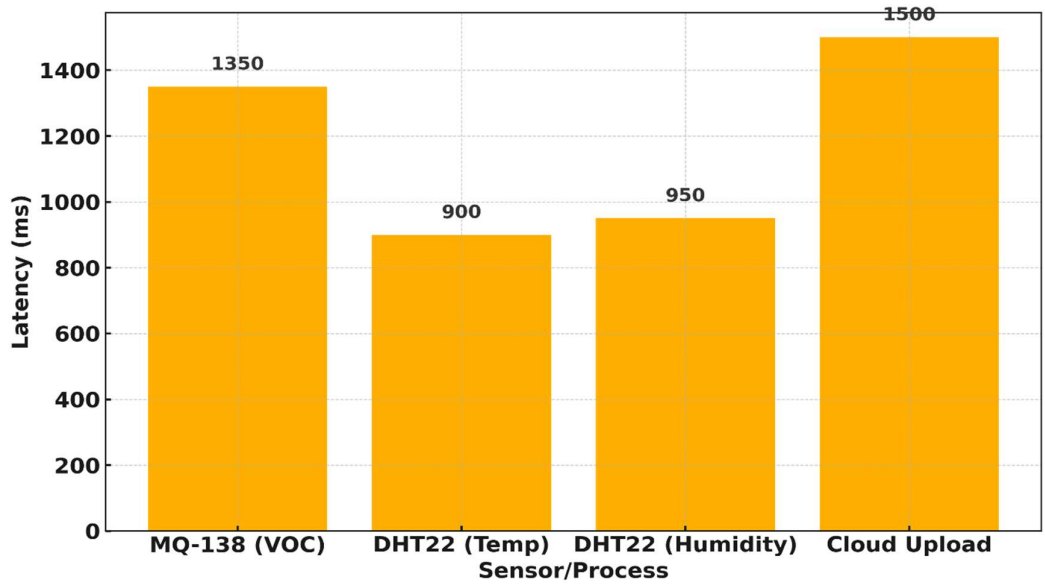

Fig. 12: Time delay in sensor feedback.

is incurred when refreshing all data completely), this delay is deemed acceptable in the context of adsorption process monitoring, where a delay of min to hours can be tolerated because these processes develop in the system on a time scale of days to weeks. No major data dropout or loss was observed during the 8-h continuous operation, and the quality of the sensor hardware and cloud communication pipeline can be considered very stable. The stability of the sensor was also proven by reading it repeatedly under controlled conditions in the chamber. MQ-138 The sensor exhibited a drift of -1.5 ppm to 4 ppm using 10 consecutive values in 100 ppm constant input, whereas DHT22, the sensor, had a negligible variation (<0.4°C and <1.5%) in repeated trials. These findings confirm that the implemented sensors are appropriate for the real-time monitoring of VOCs because they are precise and repeatable. In contrast, earlier studies reported a latency of up to 8-10 seconds with GSM modules and simple microcontrollers to sense the environment. Likewise, the poor stability characteristics of low-cost VOC D sensors are caused by power fluctuations and signal instabilities (Liu et al. 2022). These challenges are overcome by having stable 3.3V power supplies in the current system, which have 3.3V power regulators, shielded wiring, and interrupt-based polling sensor routines.

3.10. Optimization of Operating Conditions via ANN Output Mapping

In an attempt to use the trained artificial neural network (ANN) model to leverage the advantages of its predictive power for a pointwise estimation, parametric surface mapping was designed such that the most secure areas of operation could be determined in relation to the removal efficiency of VOCs. Soundly varying two important input factors, namely, VOC inlet concentration (VOC in) and inlet flow rate, while maintaining control over temperature and humidity, concerning their respective median experimental values, produced a 3D surface plot, as shown in Fig. 13, based on ANN. Fig. 13 shows the response landscape of the removal efficiency for a broad selection of input conditions. The increasing VOC value was observed to decrease the removal efficiency, implying the saturation effect of the adsorption sites of the activated carbon. At low inlet loadings (100-150 ppm), ANN indicated removal efficiencies greater than 90%, even at moderate flow rates (approximately 1.0-1.5 $L.min^{-1}$). The efficiency decreases steadily as the VOC concentration increases, even at 250 300 ppm, because there are only a fixed number of active adsorption sites per unit time, as would be expected in Langmuir-type saturation dynamics. This non-linear decimation confirms that adsorption efficiency is not only dependent on exposure but also on the temporal distribution, which is increased or decreased by the flow rate. The effect of the flow rate was non-monotonic. The efficiency is lower (by a small amount) at very low flow rates (0.5 $L.min^{-1}$) because mass transfer is restricted by diffusion. At very large flow rates (>2.0 $L.min^{-1}$), there is no time to reach equilibrium in adsorption, which leads to low efficiency. Hence, the optimum flow rate range is 1.0-1.5 $L.min^{-1}$, in which the perfection in mass transport and residence time presents maximum efficiency. This pattern is consistent with trends recorded in previous research. VOC stripping on packed beds indicated that toluene and acetone

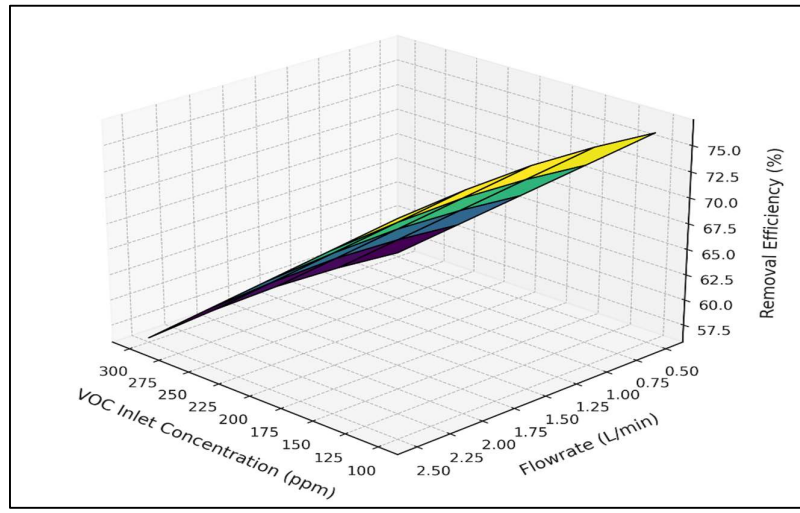

Fig. 13: 3D surface plot: VOC_in vs. flow rate vs efficiency.

stripping were most efficient near 1.2 L.min^{-1}, although increasing flow rates prematurely led to breakthrough. Similarly, another study also showed a sudden decrease in efficiency greater than 200 ppm inlet concentration with granular activated carbon, which concurred with the decay slope of this study. The surface created by ANN allows the rapid location of operational zones, and optimal results are achieved with minimum trial-and-error experimentation. It can be installed for process tuning on a dashboard that has IoT incorporated in real time (Gelles et al. 2020). For example, the system may raise an alarm when it is working close to sharp efficiency gradients, so that pre-emptive adjustment of the flow rate can be made, or the operation of further adsorption columns can be activated.

4. CONCLUSIONS

This study presents a robust and intelligent VOC removal system by synergizing experimental adsorption testing, ANN-based prediction, and IoT-enabled real-time monitoring. The packed bed column filled with activated carbon achieved a peak removal efficiency of 92.3% at a VOC concentration of 100 ppm and a flow rate of 1.0 L.min^{-1}. Breakthrough time decreased from 132 to 71 min as flow rate increased from 0.5 to 2.5 L.min^{-1}, highlighting the critical influence of residence time. The temperature gradients within the column showed a 6.3°C increase at mid-bed, indicating exothermic adsorption dynamics. The ANN model (4–8–1) achieved strong prediction fidelity with $R^2 = 0.987$, RMSE = 1.82, and MAE = 1.34, outperforming models reported in the recent literature. The learning curve analysis confirmed minimal overfitting, and the scatter plots showed a close alignment between the experimental and predicted outputs. IoT integration ensured real-time visibility, with a dashboard response latency of less than 1.5 s and sensor stability deviations of less than ±5 ppm. This study provides an effective and smart VOC elimination system through the combination of adsorption experiments, ANN-powered prediction, and real-time monitoring using the IoT. The packed bed column containing activated carbon reached a maximum removal efficiency of 92.3% at a concentration of 100 ppm of VOC and a flow rate of 1.0 L.min^{-1}. The learning curve analysis proved a low level of overfitting, and the scatter plots revealed the proximity between the experimental and predicted values. The integration of IoT allowed real-time viewing, sensor deviations not exceeding ±5 ppm, and a dashboard response time shorter than 1.5 s. The system reliability was also confirmed, as it operated without breaking during long cycles. Based on these major findings, the feasibility of ANN-IoT-based adsorption systems that are scalable is validated, providing a blueprint for the deployment of adaptive air purification units in industrial applications, where precise forecasting and automated optimization play an important role in the sustainable removal of VOCs.

5. LIST OF ABBREVIATIONS

Abbreviation	Full Form
VOC	Volatile Organic Compound
ANN	Artificial Neural Network
IoT	Internet of Things
HAP	Hazardous Air Pollutant
WHO	World Health Organization

EPA	Environmental Protection Agency
PM2.5	Particulate Matter $\leq$2.5 Microns
MQ-138	Metal Oxide Semiconductor Gas Sensor (for VOCs)
DHT22	Digital Humidity and Temperature Sensor
RMSE	Root Mean Square Error
MAE	Mean Absolute Error
R^2	Coefficient of Determination
ESP8266	Wi-Fi Microcontroller Unit (used in NodeMCU)
PPM	Parts Per Million
MOF	Metal-Organic Framework
BPNN	Backpropagation Neural Network
GAC	Granular Activated Carbon
FFNN	Feedforward Neural Network
CPU	Central Processing Unit
GUI	Graphical User Interface

6. REFERENCES

Awad, R., Haghighat Mamaghani, A., Boluk, Y. and Hashisho, Z., 2021. Synthesis and characterization of electrospun PAN-based activated carbon nanofibers reinforced with cellulose nanocrystals for the adsorption of VOCs. *Chemical Engineering Journal*, 410, p.128412. [DOI]

Chauhan, M. and Sahoo, D.R., 2024.Towards a greener tomorrow: exploring the potential of AI, blockchain, and IoT in sustainable development. *Nature Environment and Pollution Technology*, 23(2), pp.1105–1113. [DOI]

Choi, J.-S., Lim, S.-H., Lingamdinne, L.P., Park, S.Y., Koduru, J.R., Yang, J.-K. and Chang, Y.Y., 2023.Development of ultra-high surface area polyaniline-based activated carbon for the removal of volatile organic compounds from industrial effluents. *Environmental Pollution*, 337, p.122594. [DOI]

Davarpanah, M., Hashisho, Z., Crompton, D., Anderson, J.E. and Nichols, M., 2020. Modeling VOC adsorption in lab- and industrial-scale fluidized bed adsorbers: effect of operating parameters and heel build-up. *Journal of Hazardous Materials*, 400, p.123129. [DOI]

de Andrade, R.C., Menezes, R.S.G., Fiuza-Jr, R.A. and Andrade, H.M.C., 2021. Activated carbon microspheres derived from hydrothermally treated mango seed shells for acetone vapor removal. *Carbon Letters*, 31(4), pp.529–541. [DOI]

Dong, N., Wang, Z., Wang, J., Li, S., Liu, S., Wang, Y., Zhang, Y., Zhang, X. and Zhang, L., 2024. Preparation of CPVC-based activated carbon spheres and insight into the adsorption-desorption performance for typical volatile organic compounds. *Environmental Pollution*, 343, p.123177. [DOI]

Gelles, T., Krishnamurthy, A., Adebayo, B., Rownaghi, A. and Rezaei, F., 2020. Abatement of gaseous volatile organic compounds: A material perspective. *Catalysis Today*, 350, pp.46–63. [DOI]

Hou, B., Zhao, Y., Sun, W., Lu, S. and Chen, S., 2021. Glycine-based modification of activated carbons for VOCs adsorption. *Chemical Engineering Journal Advances*, 7, p.100126. [DOI]

Jurkiewicz, M., Musik, M. and Pełech, R., 2022. Competitive adsorption of a binary VOC mixture from the gas phase onto activated carbon modified with malic acid. *Industrial & Engineering Chemistry Research*, 61(3), pp.988–999. [DOI]

Kim, S., Kim, S. and Lee, S., 2023. Activated carbon modified with polyethyleneimine and MgO: better adsorption of aldehyde and production of regenerative VOC adsorbent using a photocatalyst. *Applied Surface Science*, 631, p.157565. [DOI]

Kim, T., Yoo, K., Kim, M.G. and Kim, Y.H., 2022. Photo-regeneration of zeolite-based volatile organic compound filters enabled by tio□ photocatalyst. *Nanomaterials*, 12(17), p.2959. [DOI]

Lamplugh, A., Nguyen, A. and Montoya, L.D., 2020. Optimization of VOC removal using novel, low-cost sorbent sinks and active flows. *Building and Environment*, 176, p.106784. [DOI]

Lashaki, M.J., Kamravaei, S., Hashisho, Z., Phillips, J.H., Crompton, D., Anderson, J.E. and Nichols, M., 2023. Adsorption and desorption of a mixture of volatile organic compounds: impact of activated carbon porosity. *Separation and Purification Technology*, 314, p.123530. [DOI]

Lee, J.H., Jeon, E., Song, J.-K., Son, Y., Choi, J., Khim, S., Kim, M. and Nam, K.-H., 2023a. Adsorption phenomenon of VOCs released from the fiber-reinforced plastic production onto the carbonaceous surface. *Polymers*, 15(7), p.1640. [DOI]

Lee, Y.K., Kim, H.J., Park, S.M. and Choi, D.Y., 2023b.Volatile organic compounds and metals adsorption capacity of wood bark-based activated carbons. *Wood Research*, 68(2), pp.360–375. [DOI]

Ligotski, R., Gilles, K.D., Roehnert, M., Sager, U., Asbach, C. and Schmidt, F., 2021. In-situ desorption of indoor relevant VOC toluene and limonene on activated carbon-based filter media using high relative humidity. *Building and Environment*, 191, p.107556. [DOI]

Liu, X., Ghosh, S., Liu, Y. and Wang, P., 2022. Towards integrated design and operation of complex engineering systems with predictive modeling: state-of-the-art and challenges. *Journal of Mechanical Design*, 144(9), p.091403. [DOI]

Mironenko, Y.V. and Khalyasmaa, A.I., 2023. Maintenance optimization within the lifecycle management of the gas compressor's electric motors. In: *Proceedings of the International Conference of Young Specialists on Micro/Nanotechnologies and Electron Devices (EDM)*, Novosibirsk, Russia, pp.1-5. [DOI]

Mirzaie, M., Talebizadeh, A.R. and Hashemipour, H., 2021. Mathematical modeling and experimental study of VOC adsorption by pistachio shell–based activated carbon. *Environmental Science and Pollution Research*, 28(3), pp.3125–3138. [DOI]

Mottaghitalab, A., Khanjari, A., Alizadeh, R. and Maghsoudi, H., 2021. Prediction of affinity coefficient for estimation of VOC adsorption on activated carbon using V-Matrix regression method. *Adsorption*, 27(6), pp.1159–1170. [DOI]

Roegiers, J. and Denys, S., 2021. Development of a novel type of activated carbon fiber filter for indoor air purification. *Chemical Engineering Journal*, 417, p.128109. [DOI]

Saadattalab, V., Wu, J., Tai, C.W., Bacsik, Z. and Hedin, N., 2023. Adsorption of volatile organic compounds on activated carbon with included iron phosphate. *Carbon Trends*, 11, p.100259. [DOI]

Sessa, F., Merlin, G. and Canu, P., 2022. Pine bark valorization by activated carbons production to be used as VOCs adsorbents. *Fuel*, 318, p.123346. [DOI]

Tahara, Y., Azim, M.M., Takishima, S. and Ushiki, I., 2023. Measurement and modeling of adsorption equilibria of ketone VOCs on activated carbon in supercritical co_2. *Journal of Supercritical Fluids*, 203, p.106079. [DOI]

Tzanakopoulou, V.E., Pollitt, M., Castro-Rodriguez, D., Costa, A. and Gerogiorgis, D.I., 2023. Dynamic modeling, simulation and theoretical performance analysis of volatile organic compound (VOC) abatement systems in the pharma industry. *Computers & Chemical Engineering*, 174, p.108248. [DOI]

Ushiki, I., Ueno, Y., Takishima, S., Ito, Y. and Inomata, H., 2022. Adsorption equilibria of ester vocs (ethyl and butyl acetates) on activated carbon in supercritical co2: measurement and modeling by the Dubinin–Astakhov equation. *Journal of Supercritical Fluids*, 189, p.105719. [DOI]

Wen, C., Liu, T., Wu, D., Wang, Y., Chen, H., Luo, G., Zhou, Z., Li, C. and Xu, M., 2023.Biochar as the effective adsorbent to combustion gaseous pollutants: preparation, activation, functionalization and the adsorption mechanisms. *Progress in Energy and Combustion Science*, 99, p.101098. [DOI]

Yang, J., Chen, Y., Cao, L., Guo, Y. and Jia, J., 2012. Development and field-scale optimization of a honeycomb zeolite rotor concentrator/ recuperative oxidizer for the abatement of volatile organic carbons from the semiconductor industry. *Environmental Science & Technology*, 46(1), pp.288–295. [DOI]

Zhao, Z., Wu, W., Li, W., Zhang, Z., Liu, X., Zhang, Y., Zhang, W., Zhang, L. and Hao, Z., 2024. Thermosetting phenolic resin-derived activated carbon fibers for volatile organic compound adsorption: electrospinning, preoxidation, and carbonization. *ACS ES&T Engineering*, 4(7), p.100060. [DOI]